

Nonlinear interactions as precursors to mode jumps in resonant acoustics

Praveen Panickar^{a)}

Fluid Dynamics Research Center, 10 W 32nd Street, Engineering 1 Building, Mechanical, Materials and Aerospace Engineering (MMAE) Department, Illinois Institute of Technology, Chicago, Illinois 60616

K. Srinivasan

Fluid Dynamics Research Center, 10 W 32nd Street, Engineering 1 Building, Mechanical, Materials and Aerospace Engineering (MMAE) Department, Illinois Institute of Technology, Chicago, Illinois 60616 and Department of Mechanical Engineering, Indian Institute of Technology Madras, Chennai 600 036, India

Ganesh Raman

Fluid Dynamics Research Center, 10 W 32nd Street, Engineering 1 Building, Mechanical, Materials and Aerospace Engineering (MMAE) Department, Illinois Institute of Technology, Chicago, Illinois 60616

(Received 18 January 2005; accepted 29 June 2005; published online 12 September 2005)

This paper examines instability mode switching in various supersonic jet configurations that involve resonant acoustics. Resonant acoustics includes situations where flow instabilities are enhanced by feedback. The pressure spectra in such situations are rich in multiple modes, and mode switching can occur rather unpredictably. Our experiments reveal that mode switching and the number of nonlinear interactions are interconnected and this number increases just prior to a mode switch. We quantified nonlinear interactions by counting the number of such interactions occurring over a threshold level in the nonlinear cross-bicoherence spectrum and confirmed that nonlinear interactions are precursors to mode jumps. Further, this result was found to be independent of the threshold level. Moreover, if more than one instability mode coexisted, the decay of one and the persistence of the other caused a similar increase in nonlinearities. On the other hand, if there was no mode switch, the nonlinearities remained at comparable limits over the entire operating range. The latter part of the work focused on why difference interactions significantly outnumbered sum interactions in the spectra of shock-containing resonant flows. Using linear stability calculations it is shown that most of the difference interactions that occurred had a positive spatial growth rate and were, hence, unstable. In contrast, a majority of the sum interactions lay outside the amplified region which indicated that they tend to decay spatially. © 2005 American Institute of Physics.

[DOI: [10.1063/1.2008995](https://doi.org/10.1063/1.2008995)]

I. INTRODUCTION

A. Background and motivation

This paper applies higher-order methods to study the phenomenon of instability mode switching in screeching jets and multijet coupling. Mode switching is a very unpredictable phenomenon and is still not very clearly understood. Although there are many qualitative means of observing mode switching (schlieren visualization or microphone spectra), a clear quantitative indicator does not exist. Moreover, acoustic studies have traditionally been carried out using linear spectral analysis techniques of one- and two-point measurements in the jet flowfield. Resonant acoustics mechanisms in supersonic jets can involve single or multiple jets exhibiting complex exit geometries, nonuniform shock-cell structures, or multiple modes of high amplitude. When such parameters are involved, either individually or in a combination, one would expect that linear analysis alone would not suffice to completely describe the underlying physics. For

this purpose, a higher-order technique would be required for a complete description of the mechanism. It must be noted that in this paper the terms “nonlinear spectral analysis” and “higher-order spectral analysis” have been used synonymously. A thorough analysis of a variety of resonant acoustics situations pertaining to screeching jets and multijet configurations justifies the use of a metric that we call the “nonlinear interaction density” as a quantitative precursor to the presence of a mode switch/decay. For a variety of flow situations, it has been shown that this metric faithfully serves as an indicator and precursor of the presence of a mode switch/decay.

The flow situations that we have chosen to examine consist of shock-containing flows undergoing resonant acoustics. This resonant acoustics occurring in a shock-containing jet is referred to as “jet screech” and can be summarized as follows. When disturbances in the shear layer of a shock-containing jet travel along the shock train, they interact with the shock cells to produce acoustic waves that propagate upstream. There they interact with the nascent hydrodynamic disturbances formed at the nozzle lip, thereby completing a

^{a)}Author to whom correspondence should be addressed. Fax: (312) 567-7230. Electronic mail: panipra@iit.edu

feedback loop. The resultant high amplitude acoustic wave phenomenon produced is called jet screech. Jet screech was first discovered by Powell¹ in the early 1950s when studying jets from nozzles with a two-dimensional exit using the toepfer-schlieren technique. In spite of all the advances made in screech instability frequency prediction, as well as in the physical understanding of the phenomenon, the occurrence of multiple modes and their switching is still unpredictable, and is the focus of our work.

B. Review of relevant literature

There is a wealth of literature available that characterizes and quantifies the nature and occurrence of jet screech using single- and two-point measurements. Both single as well as twin jets having axisymmetric or plane exit geometries have been studied earlier in great detail. An exhaustive review of the voluminous work in this field is given by Raman.² The next couple of subsections enumerate the work in literature that use both linear and nonlinear techniques, and the contributions therein that are relevant to the work presented in this paper.

1. Screech studies on single and twin jets using linear spectral analysis

Axisymmetric jets have been very closely studied in the past by many researchers. Powell³ was among the first to study axisymmetric, shock-containing jets in some detail and found that there were certain regions where the frequency varied steadily, but these regions could be separated by regions of instability, or by sudden transitions between the regions. These regions were called stages or modes and labeled A–D. Following him, Merle⁴ used high-speed stroboscopic lighting to study the various stages of the screech frequency and additionally reported (as quoted in the work of Powell, Umeda, and Ishii⁵) that stage A could be divided into two parts: A_1 which was unstable and A_2 which was stable. Additionally, stage B was unstable, stage C was stable, and stage D was unstable and not always visible. Merle⁴ also reported the existence of weak periodicities that appeared to be the continuations of the labeled stages.

Following the early work, a lot of researchers studied the physics of axisymmetric jets. Norum⁶ demonstrated that more than one instability mode could coexist for a given nozzle pressure ratio (NPR) over most of the Mach number range tested. As far as twin axisymmetric jets are concerned, Seiner, Manning, and Ponton⁷ studied the dynamic pressure fluctuation in the internozzle region of a B1-B aircraft. Wlezien⁸ studied the effect of internozzle spacing on the interaction between supersonic jets and concluded that the noise produced was strongly dependent on the internozzle spacing and the fully expanded jet Mach number. Shaw⁹ studied various techniques for noise suppression in twin axisymmetric jets. Morrison and McLaughlin¹⁰ and Hu and McLaughlin¹¹ studied underexpanded supersonic jets and observed that there were considerable differences between the spectra of low and high Reynolds number jets. Recent advances in measurement techniques have helped in illuminating the physics of compressible flow. Yüceil, Ötügen, and

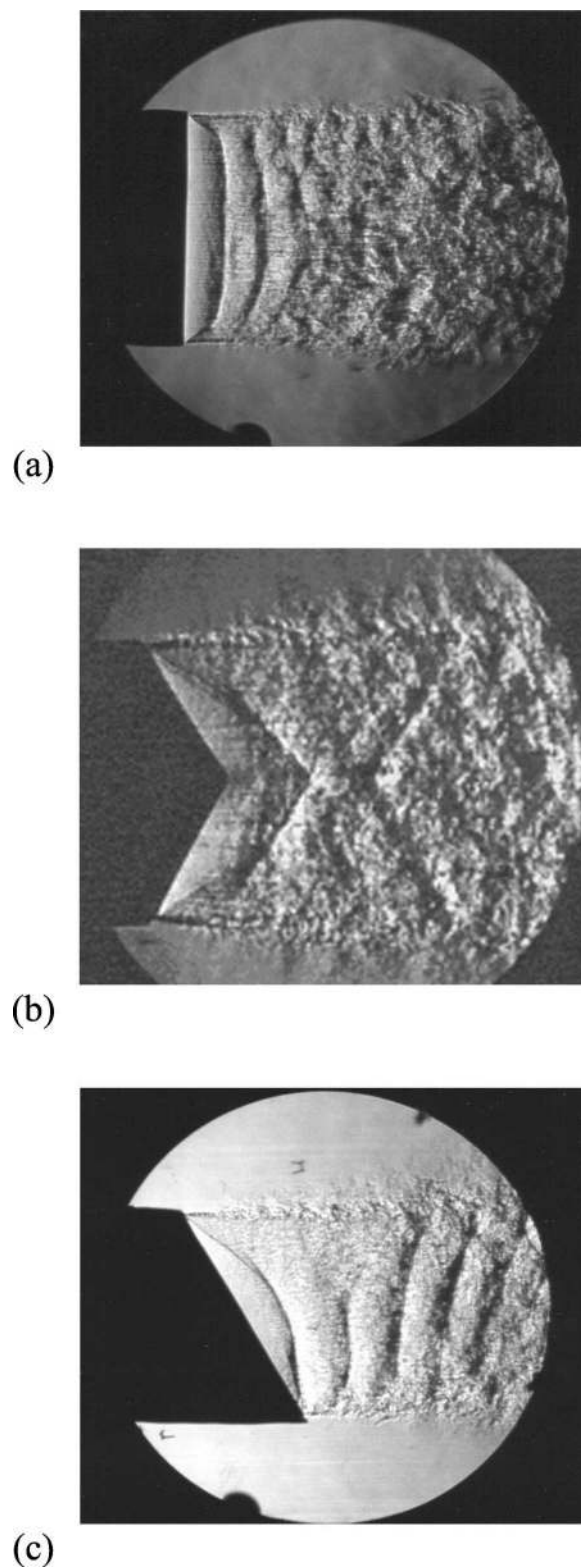


FIG. 1. Schlieren images of shock-containing jets illustrating various spanwise (a) symmetric, (b) antisymmetric, and (c) oblique modes from Raman (Ref. 16).

Arik¹² used particle image velocimetry (PIV) and Thurow, Hileman, Samimy, and Lempert¹³ used real time laser flow visualization to study high-speed flows. Yüceil and Ötügen¹⁴ developed scaling parameters for underexpanded supersonic jets. Zaman¹⁵ studied the spreading rate of initially com-

pressible jets. However, despite these advances, the prediction of mode jumps in unsteady flows has remained an elusive goal.

Flows from rectangular nozzles have received attention in the recent past due to their potential advantages in thrust vectoring applications. Raman¹⁶ studied the screech tones from rectangular convergent-divergent rectangular jets having three different exit geometries: uniform straight edge, single beveled, and double beveled exits. Figure 1 shows the shock-cell structure of rectangular jets having various exit geometries (taken from Raman¹⁶). It is immediately apparent that whereas the uniform exit rectangular nozzles and the double beveled exit nozzles produce jets with shock-cells that are spanwise symmetric about the jet centerline, the shock cell structure of jet from the single beveled nozzle, as expected, does not show any such symmetry. It was possible to identify three types of spanwise instability modes: symmetric (spanwise phase difference $\sim 0^\circ$), antisymmetric (spanwise phase difference $\sim 180^\circ$), and oblique (spanwise phase difference neither 0° nor 180°). More than one mode could be simultaneously present at certain operating conditions and by the use of an instantaneous spectrum, represented as a waterfall chart, it was possible to distinguish whether the two modes were coexisting or mutually exclusive. Prior to this, Raman and Rice¹⁷ had studied the instability modes of a regular exit convergent rectangular jet using hot films and microphones to characterize the axial evolution of the hydrodynamic instability modes. Tam, Shen, and Raman¹⁸ showed that the screech frequency of nozzles with two-dimensional exits could be predicted using the waveguide approach. Raman¹⁹ observed that in plane jets with a uniform exit, that are significantly underexpanded, the screech phenomenon ceased to exist and concluded that this was caused due to aerodynamic blockage of the feedback process by the excessive expansion of the jet at the nozzle exit that occurs at higher stages of underexpansion. Kim and Samimy²⁰ and Kerechanin, Samimy, and Kim²¹ studied the effects of modifications to the trailing edge of uniform exit rectangular nozzles as a means to characterize the noise radiation emanating therefrom. Raman and Taghavi²² studied the coupling of twin jets of rectangular geometry and found that the jets coupled either symmetrically or antisymmetrically in the spanwise direction. Raman²³ revisited the coupling problem to study the characteristics of twin jets emanating from nozzles having a double beveled exit and demonstrated that the jets from these complex exit geometry nozzles exhibited the same types of coupling instability modes as those of jets from uniform exit nozzles.

More recently, the authors of the present work studied the interaction between twin jets from nozzles with single beveled exits²⁴ (bevel angle = 30°). They found that when operated individually, the jets exhibited spanwise symmetric, antisymmetric, and oblique instability modes. When these nozzles were operated in the twin configuration, there were two configurations that were possible; viz., the contradirected (or “arrowhead-shaped”) configuration or the codirected (or “V-shaped”) configuration. It was found that the former configuration exhibited no spanwise coupling instability modes. However, in the codirected configuration, the jets were coupled and exhibited only the spanwise symmetric and spanwise antisymmetric instability modes. Another related recent study by Joshi, Srinivasan, and Raman²⁵ examined the effects of nozzle yaw orientation on the coupling mechanism. This study brought to light the coupling mechanism of twin jets having uniform exits, and single beveled exits with two bevel angles (10° and 30°) and in two configurations (codirected and contradirected), under various yaw configurations.

2. Screech studies on single and twin jets using nonlinear spectral analysis

As mentioned earlier, nonlinear spectral analysis techniques have the potential to uncover jet interaction intricacies that have eluded researchers for a long time. For this paper, the higher-order term we use is the cross-bicoherence (CBC). The cross bicoherence is obtained by normalizing the cross bispectrum, which is an ensemble average obtained from the discrete Fourier transforms of two discrete timeseries signals. The discrete cross-bispectrum for an ensemble k , ($S_{YXX}^{(k)}$), can be expressed by Eq. (1) as follows:

$$S_{YXX}^{(k)}(f_1, f_2) = Y^{(k)}(f_1 + f_2) X^{(k)*}(f_1) X^{(k)*}(f_2), \quad (1)$$

where $X^{(k)}(f)$ and $Y^{(k)}(f)$ are the discrete Fourier transforms of the timeseries signals $x(t)$ and $y(t)$ and f is the frequency. The discrete cross-bispectrum, (S_{YXX}), is obtained by taking an ensemble average of Eq. (1) and can be expressed as shown in Eq. (2),

$$S_{YXX}(f_1, f_2) = \frac{1}{M} \sum_{k=1}^M S_{YXX}^{(k)}(f_1, f_2). \quad (2)$$

Finally, the cross-bicoherence spectrum is obtained by normalizing Eq. (2) using the power spectrum of each of the two signals and the resulting expression for the cross-bicoherence b_c is given by Eq. (3):

$$b_c^2(f_1, f_2) = \frac{|S_{YXX}(f_1, f_2)|^2}{\left(\frac{1}{M} \sum_{k=1}^M |Y^{(k)}(f_1 + f_2)|^2 \right) \left(\frac{1}{M} \sum_{k=1}^M |X^{(k)}(f_1) X^{(k)}(f_2)|^2 \right)}. \quad (3)$$

TABLE I. Compilation of flow description, instability type, and mode jump considered in the present work.

Flow description	Instability mode type	Existence of mode jump	Geometry/orientation
Twin, shock-containing jets	Spanwise coupling modes	YES	Uniform exit rectangular (No yaw)
Single, shock-containing jet	Spanwise modes	YES	Single beveled rectangular
Single, shock-containing jet	Azimuthal modes	YES	Axisymmetric
Twin, shock-containing jets	Spanwise coupling modes	NO	Uniform exit rectangular (Yaw angle=15°)
Single, shock-containing jet	Spanwise modes	NO	Uniform exit rectangular

Thus, the cross-bicoherence is a third-order estimate obtained from two simultaneously acquired timeseries signals and can be considered analogous to cross-coherence in linear spectral analysis. The use of nonlinear techniques in analyzing jet flows is not new, although, it has not been as widely used as linear analysis techniques. Thomas and Chu²⁶ studied the evolution of a planar shear layer of a subsonic jet using auto- and cross-bicoherence. The auto- and cross-coherence quantities used here are higher-order analogs of the auto- and cross-spectrum quantities used in linear spectral analysis. In their work, they showed that the shear layer showed a preference for difference interactions rather than sum interactions. They also studied the axial evolutions of nonlinear interactions by studying the relative magnitudes of the interactions. Studies on the nonlinear interactions that occur in shock-containing supersonic jets were first conducted by Ponton and Seiner²⁷ followed by Walker and Thomas.²⁸

Srinivasan, Panickar, Raman, Kim, and Williams²⁹ used nonlinear spectral analysis to study twin-jet coupling. In their work, they used the cross-bicoherence spectrum to quantify the nonlinear interactions that occurred between twin supersonic jets from single beveled nozzles. They found that jets that were considered decoupled by linear spectral analysis metrics were observed to be interacting nonlinearly if higher-order spectral analysis metrics were used. In addition, the number of nonlinear interactions was quantified using a metric termed as the “interaction density,” represented as $I_{c,n}$ where n is a number between 0 and 1. The interaction density is computed by calculating the number of interactions in the cross-bicoherence spectrum that have cross-bicoherence levels greater than n , and can be mathematically expressed as

$$I_{c,n} = \sum_{i=1}^N \sum_{j=1}^M \beta_{ij}, \quad \beta_{ij} \begin{cases} =1, & b_c^2(f_i, f_j) \geq n, \\ =0, & b_c^2(f_i, f_j) < n, \end{cases} \quad (4)$$

where N and M are the numbers of discrete frequency ranges in the cross-bicoherence spectrum. Srinivasan, Panickar, Raman, Kim, and Williams²⁹ found that there was an abrupt increase in the number of nonlinear interactions when a mode switch occurred. In the present work we examine the connection between mode jumps and the number of nonlinear interactions in several resonant acoustics situations.

C. Objectives

The main objectives of the present study are stated as follows.

- (1) Study the effect of instability mode switch/decay on the number of nonlinear interactions for various resonant acoustics flow situations. The various flow situations include different shock-cell structures, instability mode types, and jet orientations.
- (2) Use concepts from linear stability analysis to explain why difference interactions outnumber sum interactions when multiple modes in shock-containing flows interact.

For the first point mentioned above, the authors studied the nonlinear interactions and instability modes for a variety of shock-containing jets that had both mutually exclusive as well as coexisting instability modes (compiled in Table I) as described below.

- (1) Twin, shock-containing plane jets with uniform shock cells.
- (2) Single, shock-containing plane jet with oblique shock cells.
- (3) Single, shock-containing axisymmetric jet.
- (4) Twin, shock-containing plane jets with uniform shock cells, yawed at 15°.
- (5) Single, shock-containing plane jet with uniform shock cells.

It must be noted that plane jets refer to jets that have a rectangular exit. Uniform shock cells refer to jets emanating from uniform rectangular exits and oblique shock cells refer to jets emanating from single beveled rectangular exits. In order to meet the second objective, the authors considered the nonlinear spectra for the following cases:

- (1) Twin, shock-containing plane jets with oblique shock cells, yawed at 10°, in the contradirected configuration.
- (2) Twin, shock-containing plane jets with oblique shock cells, yawed at 20°, in the contradirected configuration.

II. EXPERIMENTAL METHODOLOGY AND UNCERTAINTY

Unsteady pressure data in the nearfield were obtained using two-point microphone measurements. The microphones were located at the spanwise centers of the nozzles for the twin-jet configurations and at the spanwise extremities of the nozzle for the single jet configuration. For the axisymmetric jet, there were four microphones located on the periphery of the nozzle separated by an azimuthal angle of

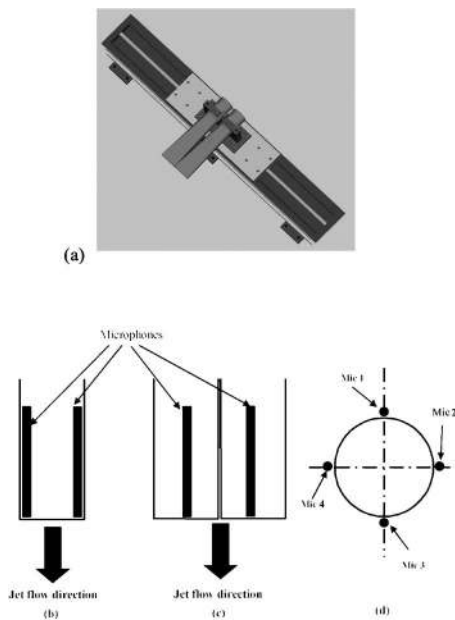


FIG. 2. Experimental schematics. (a) Schematic of the twin-jet setup, (b) microphone arrangement for measuring spanwise instability modes in a single jet, (c) microphone arrangement for measuring spanwise coupling instability modes in twin jets, and (d) microphone arrangement for measuring azimuthal instability modes in an axisymmetric jet (direction of jet flow is out of the plane of the paper).

90°. All the experiments corresponding to the data analyzed were performed in the High Speed Jet Facility of the Fluid Dynamics Research Center at the Illinois Institute of Technology. A detailed description of the test facility can be obtained from Panickar, Srinivasan, and Raman²⁴ and will not be repeated here. All acoustic data were acquired using $\frac{1}{4}$ -in. Brüel & Kjær microphones and associated preamplifiers and signal conditioners. A schematic of the setup for twin jets is shown in Fig. 2(a). As shown, the nozzles were mounted on separate carriages of a traversing mechanism. Each carriage rests on leadscrews with opposite hand threads. The motors of the leadscrew are computer controlled which allows the user to change the internozzle separation. For changing the orientation of the jets, the nozzles were further mounted on rotary tables which are also computer controlled and can be adjusted to change the yaw orientation between the nozzles. Also shown in the figure is a schematic of the microphone locations for the single and twin plane jet configurations [Figs. 2(b) and 2(c), respectively] and the single axisymmetric jet configuration [Fig. 2(d)]. All analog signals acquired through the connector board were digitized using a 12-bit National Instruments card. The programming interface for communicating with the card as well as for controlling the traversing mechanism was LABVIEW. Postprocessing of the timeseries data acquired was done using MATLAB.

The experimental uncertainties for the experiments are restricted to errors in measuring the sound pressure levels (SPLs) and the frequencies. The uncertainty in the SPLs is calculated to be within around 1%, including repeatability factors. The uncertainty in the frequency measurements was found to be within around 2%. The fully expanded jet Mach

number was calculated assuming an isentropic expansion from stagnation conditions in the plenum, to atmospheric conditions. The uncertainty in calculating the fully expanded Mach number is calculated to be 0.016%.

III. RESULTS AND DISCUSSION

We begin with a brief illustration of the advantage of using nonlinear spectral analysis over traditional linear spectral analysis. A detailed discussion on this aspect can be found in the work of Srinivasan, Panickar, Raman, Kim, and Williams²⁹ and hence, only a brief summary is presented in this paragraph. Figure 3(a) shows the timeseries of two synthetically generated signals. One is obtained by a linear superposition of two frequencies, at 5 kHz and 8 kHz, and the other is obtained by a quadratic modulation of the same two frequencies. As seen from the figure, the timeseries of the two signals are completely distinct. However, the power spectral density plot of the modulated signal shows peaks at 3 kHz and 13 kHz. Thus, looking at the power spectral density alone, one would be unable to detect the quadratic phase coupling between 5 kHz and 8 kHz. Figure 3(c) shows the cross-bicoherence spectrum of the two signals in a three-dimensional plot and Fig. 3(d) shows a projection of Fig. 3(c) as viewed from the top. The cross-bicoherence spectrum consists of two distinct peaks, corresponding to the frequency content in the modulated signal [3 kHz and 13 kHz, as shown in Fig. 3(d)]. Thus, higher-order spectral analysis is able to identify nonlinear interactions that cannot be detected by linear analysis alone, provided that the phase difference between the modulated signals is small (for an explanation regarding the role of phase difference in cross-bicoherence spectrum, see Ref. 29). It is a limitation of cross-bicoherence that it reveals quadratic interactions only when there is phase coherence between the interacting modes. However, in the case of closely spaced shock-containing jets, it is reasonable to assume that nonlinear interactions between modes occur well before they become phase incoherent, and thus justifies the use of this technique for high-speed jet modal interaction studies. In summary, linear spectral techniques eliminate the phase information in a signal which could be essential for understanding the physics behind complex phenomena, such as the ones being studied in this paper.

A. Nonlinear interactions and mode switching in shock-containing jets

In the work of Srinivasan, Panickar, Raman, Kim, and Williams,²⁹ a metric called the “interaction density” [Eq. (4)], which was indicative of the amount of nonlinearity in a signal, was successfully used. In their work, they looked at the interactions occurring between twin jets with oblique shock cells in the codirected configuration. One of the main conclusions from their work was that there appeared to be a strong correlation between a switch in the coupling mode and the interaction density. They noticed that around the fully expanded jet Mach numbers where the spanwise coupling mode switched from symmetric to antisymmetric the nonlinear interaction density peaked as compared to the interaction density for conditions where there was no mode

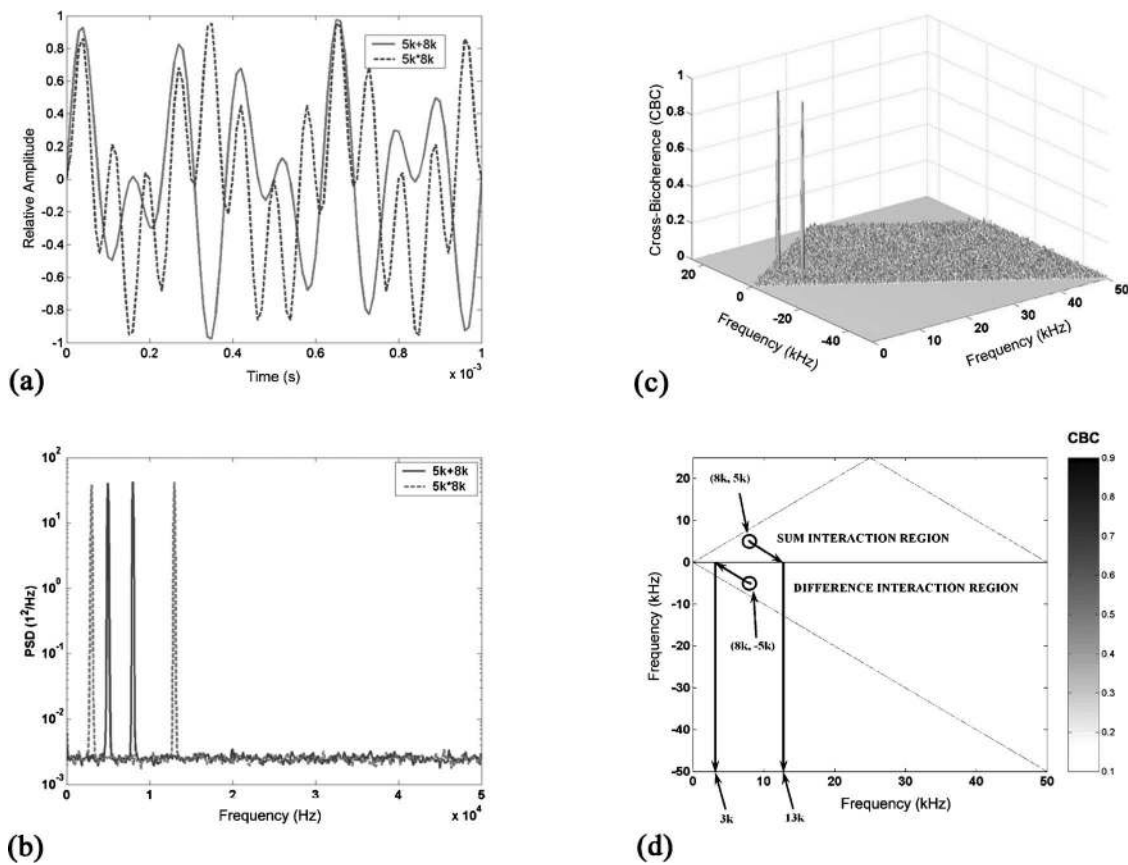


FIG. 3. Limitations of linear spectral analysis. (a) Timeseries for two different types (linearly superposed and quadratically modulated) of signals containing frequencies of 5 kHz and 8 kHz. (b) Power spectral density plots for the timeseries shown in (a) indicate that while linear spectral analysis is adequate for linearly superposed signals, it misrepresents quadratically modulated signals. (c) Three-dimensional cross-bicoherence spectrum for the timeseries shown in (a) showing two spikes indicating the frequency content of the modulated signal. (d) Projection of the cross-bicoherence spectrum shown in (c) when viewed from the top.

switch. In the present paper, we investigate the connection between mode switching and number of nonlinear interactions for several resonant acoustics situations including the data from the work of Panickar, Srinivasan, and Raman²⁴ and Joshi, Srinivasan, and Raman.²⁵ Interaction densities at cut-off cross-bicoherence values of 0.3 ($I_{c,0.3}$) were obtained [using Eq. (4)] and plotted against the fully expanded jet Mach number for a particular configuration. To confirm that the trends were not dependent on the threshold value, the results for a cross-bicoherence cutoff of 0.4 ($I_{c,0.4}$) are also shown.

Figure 4 shows the results for the jets from twin, shock-containing jets with oblique shock cells, in the codirected configuration. Figures 4(a) and 4(b) show the tonal sound pressure level characteristics and the spanwise phase difference at the tonal frequency across the range of Mach numbers of operation (reproduced from Panickar, Srinivasan, and Raman²⁴). The spanwise coupling instability modes at the tonal frequency across the fully expanded Mach number range of operation can be identified from Fig. 4(b). As seen from this figure, the spanwise phase is approximately 0° at the lower Mach numbers (corresponding to twin-jet sound pressure levels that were greater than the single jet sound pressure levels) which indicates the presence of a spanwise symmetric instability mode. At a fully expanded Mach number of around 1.4, the spanwise phase abruptly jumps to, and

stays at, values close to 180° which alludes to the presence of a spanwise antisymmetric instability mode. Note that at this fully expanded Mach number, the sound pressure levels for the twin jets drop from being greater than that for single jets to being lower than that of single jets. Finally, Fig. 4(c) shows the variation of the interaction density across the operating fully expanded Mach number range (reproduced from Srinivasan, Panickar, Raman, Kim, and Williams²⁹). As seen in this figure, the interaction density peaks around a fully expanded Mach number of 1.4 which agrees well with the data presented in the sound pressure level chart and the phase map of Figs. 4(a) and 4(b), respectively. The present work will examine the connection between the interaction density and the mode switch for a number of resonant acoustics situations.

1. Resonant acoustics situations with mode jump

a. Twin, shock containing rectangular jets with uniform shock cells. In the present work, we began by examining two separate cases from the work of Joshi, Srinivasan, and Raman²⁵ that studied the effect of yaw on twin-jet coupling. First, the data for twin jets with uniform shock cells, without any yaw, were analyzed. Figures 5(a) and 5(b) show the sound pressure level variation and frequency variation, re-

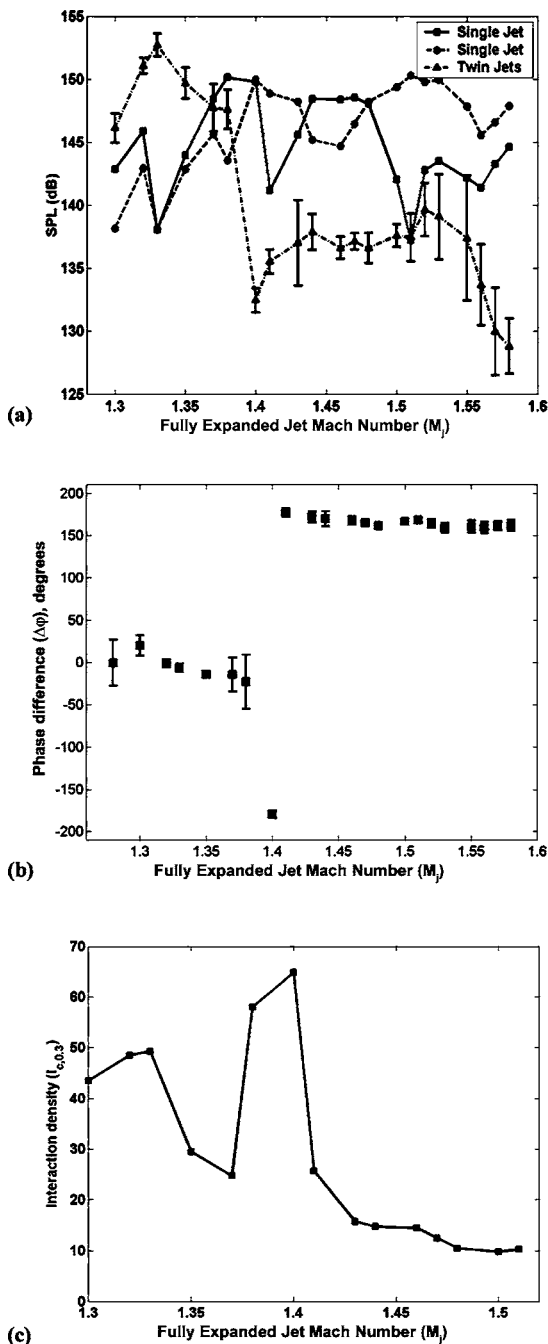


FIG. 4. Linear and nonlinear characteristics of twin jets from single beveled nozzles (bevel angle = 30°) in the codirected configuration. Data from Panickar, Srinivasan, and Raman (Ref. 24) for (a) and (b) and from Srinivasan, Panickar, Raman, Kim, and Williams (Ref. 29) for (c). (a) Peak SPL variation across the Mach number range for single and twin jets. (b) Spanwise phase variation with Mach number showing an instability coupling mode jump from spanwise symmetric to spanwise antisymmetric at $M_j \approx 1.4$. (c) Variation of nonlinear interaction density with Mach number showing a sudden increase in the nonlinearity at $M_j \approx 1.4$.

spectively, for the single and twin jets across the Mach number range of operation. As seen in this chart, around a Mach number of around 1.55, the sound pressure level of the twin jets increases to become significantly greater than that for the single jets. Figure 5(c) shows the phase map for the twin jets at the tonal frequency over the range of Mach numbers tested. As seen from this graph, at the lower Mach numbers, the phase difference is approximately 180° . At the higher Mach numbers, the phase difference is seen to be approximately 0° . The shift from a spanwise antisymmetric mode to a spanwise symmetric mode is seen to occur at around a fully expanded Mach number of 1.55 which agrees well with the sound pressure level data in Fig. 5(a). We performed a nonlinear spectral analysis on these data to calculate the interaction density. The nonlinear interaction density variation with

the fully expanded Mach number is shown in Fig. 5(d). As seen in the figure, the nonlinear interaction density peaks around a fully expanded Mach number of 1.55. Both cross-coherence cut-off values showed the same trend of nonlinear interaction density.

b. Single, shock-containing rectangular jet with oblique shock cells. Next, in order to check the variation in nonlinear interaction density for spanwise instability modes as opposed to spanwise coupling instability modes as discussed in the previous paragraph, the data for a single, shock-containing jet with oblique shock cells were analyzed. The spanwise modes were obtained by placing two microphones at the spanwise edges of the nozzle, as shown in the schematic in Fig. 2(b). Figure 6(a) shows the SPL recorded by each microphone and Fig. 6(b) shows the variation of the screech

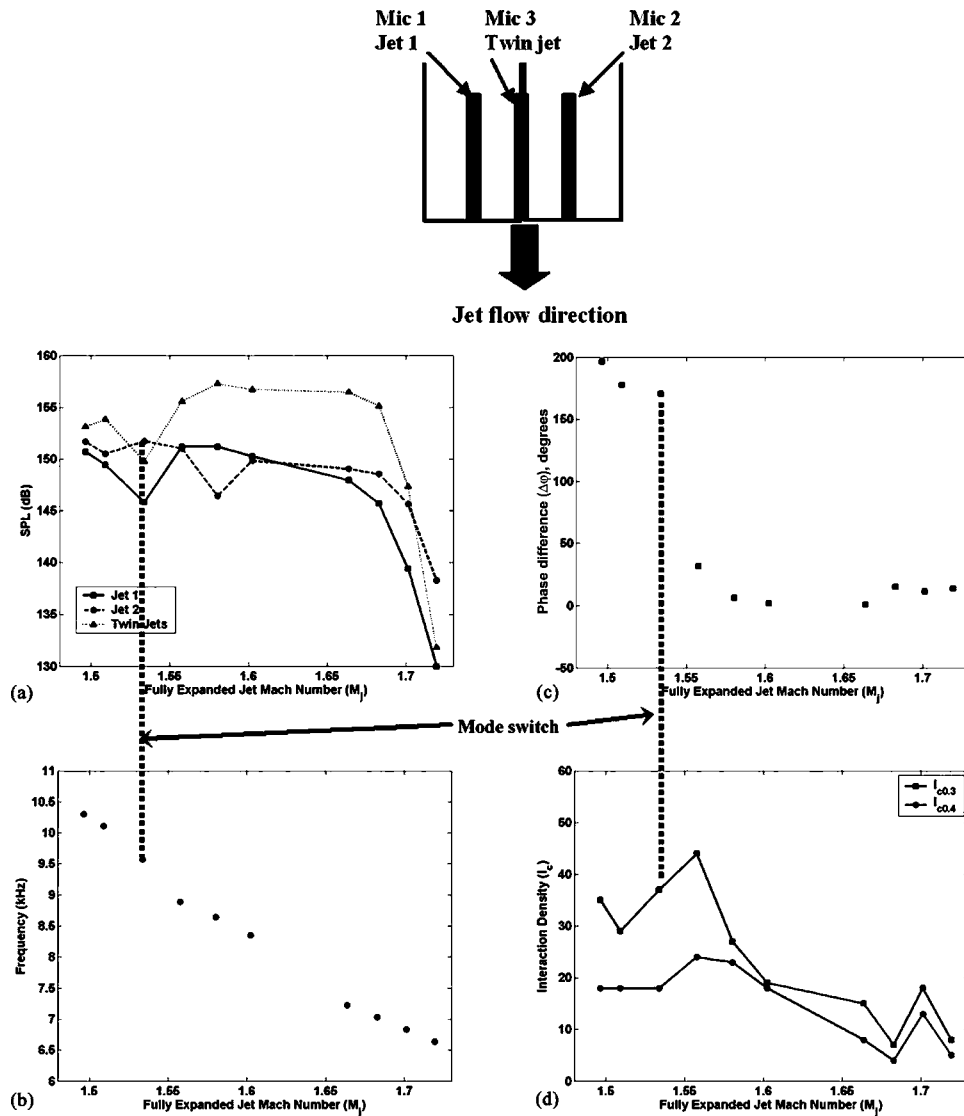


FIG. 5. Linear and nonlinear characteristics of twin jets from uniform exit rectangular nozzles. Data from Joshi, Srinivasan, and Raman (Ref. 25) for (a) and (b). (a) Peak SPL variation across the Mach number range for single and twin jets. Single jet data were acquired by operating one of the jets and measuring the SPLs recorded by the corresponding microphone and twin-jet data were acquired by operating both jets simultaneously and measuring the SPL recorded by microphone 3. (b) Variation of screech frequency with Mach number. (c) Spanwise phase variation between microphone 1 and microphone 2 with Mach number. (d) Variation of nonlinear interaction density with Mach number considering two cut-off cross-bicoherence thresholds of 0.3 and 0.4, as shown by the two lines.

frequency across the Mach number range of operation. Figure 6(c) shows the corresponding phase chart. As seen from Fig. 6(c), the spanwise phase for the single jet remains antisymmetric for the lower operating range of fully expanded Mach numbers. However, around $M_j=1.4$, the spanwise mode suddenly shifts from antisymmetric to symmetric, after which it remains in the spanwise symmetric mode for the remainder of the operating range. The fully expanded Mach number where the mode switched was approximately the same for both single and twin jets from single beveled nozzles. This can be seen by comparing the respective phase charts [Figs. 4(c) and 6(c), respectively]. However, for the single jet, the spanwise mode shifted from antisymmetric to symmetric whereas for the twin jets, the spanwise-coupled mode shifted from symmetric to antisymmetric. Finally, Fig. 6(d) shows the variation of the nonlinear interaction density with the fully expanded Mach number. As seen, the nonlinear

interactions peak sharply around $M_j \sim 1.4$, corresponding to the spanwise phase shift. The trends of the nonlinear interaction density for both cross-bicoherence cut-off values chosen were similar which meant that the peaking phenomenon was not dependent on the value of the cut-off chosen.

c. Single, shock-containing axisymmetric jet. It is widely acknowledged that axisymmetric, shock-containing jets exhibit more complex instability modes^{4,6} (azimuthal) as opposed to plane jets (spanwise). Moreover, these modes can coexist over a range of fully expanded Mach numbers. Hence, we examined the screech characteristics of an axisymmetric nozzle using four microphones, each separated azimuthally by 90° from the other, along the periphery of the nozzle, as shown in the schematic in Fig. 2(d). At the lowest Mach numbers, the jets exhibited an axisymmetric ($m=0$) instability mode. This was determined from the phase relation between the microphones which were all in phase. The

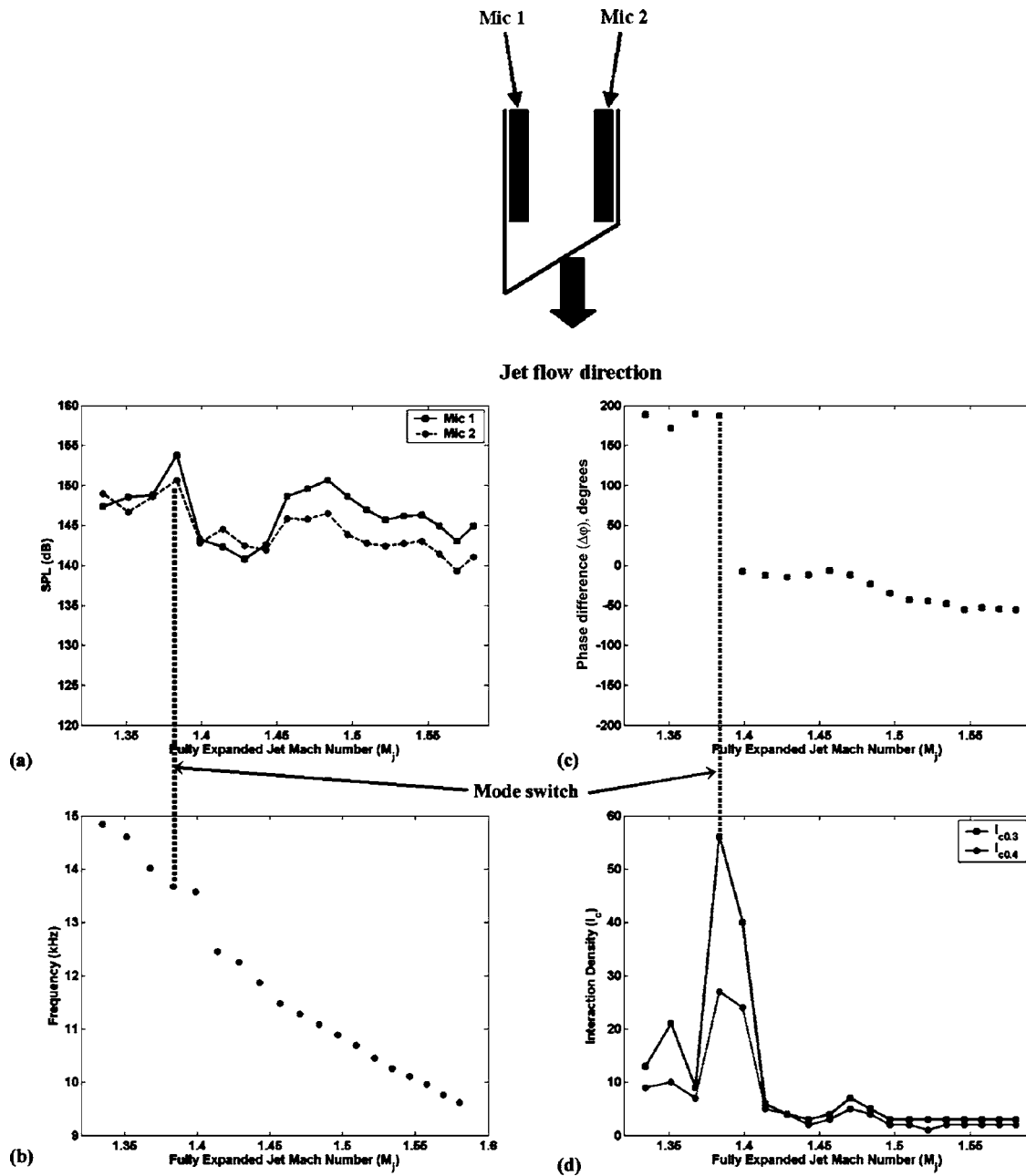


FIG. 6. Linear and nonlinear characteristics of a jet from one single beveled nozzle. (a) Peak SPL variation across the Mach number range for spanwise located microphones as shown in the schematic. (b) Variation of screech frequency with Mach number. (c) Spanwise phase variation between microphone 1 and microphone 2 with Mach number depicting the spanwise antisymmetric and spanwise symmetric instability modes. (d) Variation of nonlinear interaction density with Mach number for two different cross-bicoherence cutoffs.

axisymmetric mode persisted for a wide range of Mach numbers. Around a fully expanded Mach number of 1.16, a flapping ($m = \pm 1$) mode came into existence as seen from the phase difference between diagonal microphones (approximately 180°). Note that the $m = \pm 1$ mode is produced by the combination of equal and opposite helical modes. At a fully expanded Mach number of around 1.3, the flapping mode started decaying and around $M_j = 1.35$, the helical ($m = 1$) instability mode was observed. This was determined from the phase difference between microphone pairs 1-2, 1-3, and 1-4 which were 90° , 180° , and 270° , respectively. Figure 7(a) shows the SPL variation as recorded by microphone 1 for each of the three instability modes. For each instability

mode, the frequency corresponding to the instability varied smoothly. This variation in the instability frequency is shown in Fig. 7(b). Table II shows the phase relationship for a few representative frequencies for each instability mode type that was observed for the axisymmetric nozzle tested. It can be seen that each mode type produces a distinct phase relationship as explained earlier. Figure 7(c) shows the corresponding phase variation between microphone 1 and microphone 3 across the range of operating Mach numbers. The axisymmetric mode coexists with the flapping mode until a fully expanded jet Mach number of 1.35 after which the flapping mode ceases to exist. Thereafter, the axisymmetric mode co-

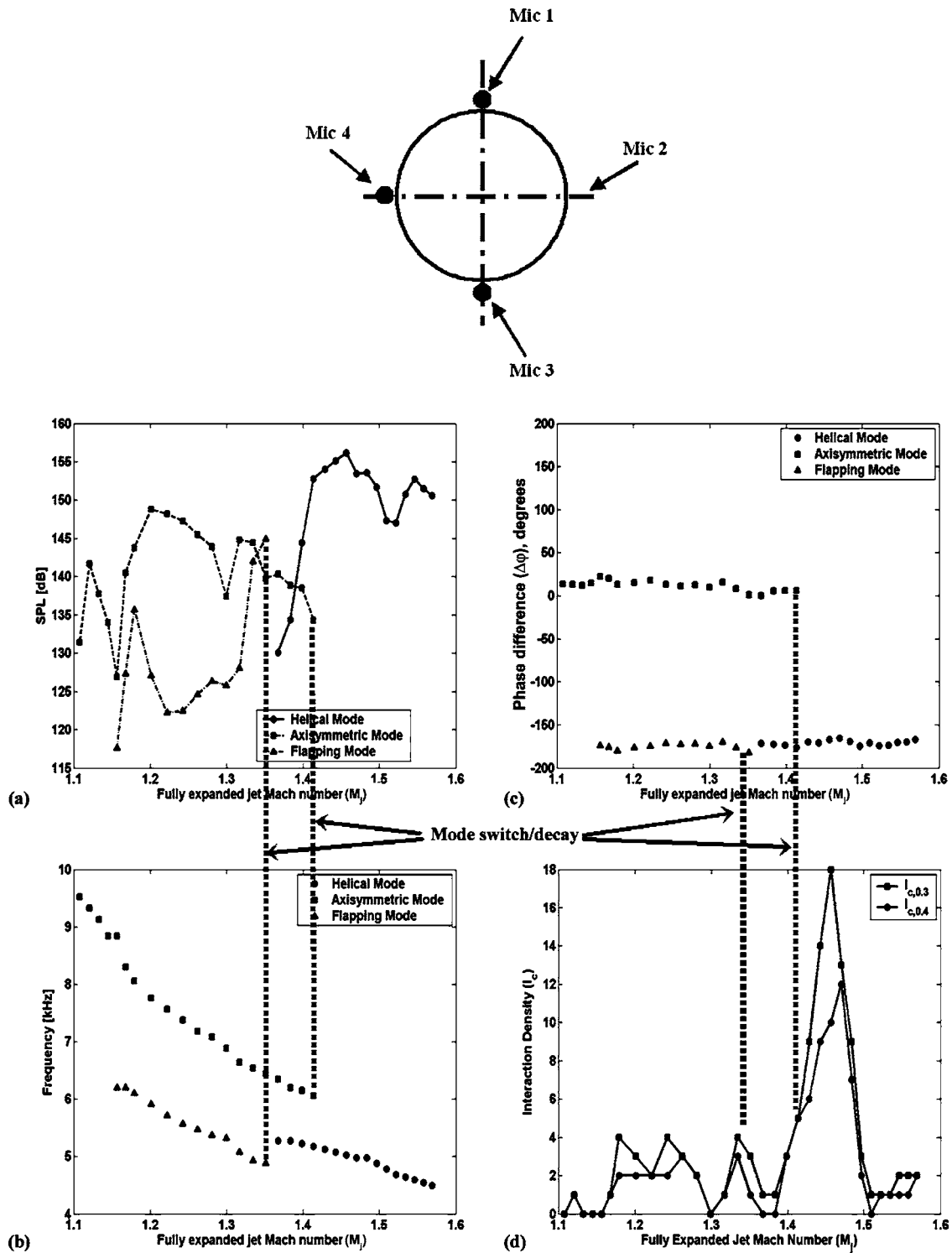


FIG. 7. Linear and nonlinear characteristics of an axisymmetric nozzle. (a) SPL variation across the Mach number range for the various modes measured using microphone 1 shown in the schematic. (b) Variation of instability frequency with Mach number. (c) Variation of the azimuthal instability mode as measured by microphone 1 and microphone 3 with the Mach number showing the various instability modes (axisymmetric, helical, and flapping). (d) Variation of nonlinear interaction density measured by microphone 1 and microphone 3 with Mach number for two separate cross-bicoherence cutoffs.

exists with the helical mode until a Mach number of 1.42 after which the axisymmetric mode ceases to exist and the helical mode persists. The focus of our work is the variation of the nonlinear interaction density [Fig. 7(d)] with Mach number. As seen, when the flapping mode ceases to exist (around $M_j \sim 1.35$) there is a slight increase in the nonlinear

interactions. However, when the axisymmetric mode ceases to exist (around $M_j \sim 1.42$) there is a marked increase in the number of nonlinearities as seen by the prominent peak in the nonlinear interaction density chart. Similar trends were observed using two different cross-bicoherence cut-off thresholds.

TABLE II. Frequency and corresponding phase differences for various instability modes seen in an axisymmetric jet. For schematic of microphone location refer to Fig. 2(d).

Instability mode type	Frequency (Hz)	Phase difference (degrees)		
		Microphones 1 and 2	Microphones 1 and 3	Microphones 1 and 4
Axisymmetric mode	9130.86	-10.25	11.7982	1.32
	8398.44	-0.67	22.1104	21.75
	8056.64	8.72	13.0098	21.78
	7568.36	-0.27	17.9854	17.70
	7177.73	5.16	11.2632	16.44
	6640.63	0.05	8.1552	15.64
Flapping mode	6103.52	18.26	-161.98	
	5957.03	8.19	-168.27	
	5517.58	4.46	-166.64	
	5419.92	6.11	-166.27	
	5371.09	7.19	-164.88	
	5273.44	9.26	-165.19	
Helical mode	5224.60	91.27	166.08	274.26
	5127.00	81.66	167.29	254.69
	5078.10	106.19	170.02	273.07
	4980.50	103.42	169.79	272.45
	4931.60	94.86	166.02	269.12
	4589.80	83.22	167.36	249.80

2. Resonant acoustics situations without mode jumps

a. Twin, shock-containing rectangular jets with uniform shock cells, yawed at 15°. For completeness, the authors looked at a data set where the spanwise mode during coupling did not show a mode jump. For this purpose, data from a previous work²⁵ for twin, shock-containing plane jets with uniform shock cells, yawed at 15°, were analyzed. Figures 8(a) and 8(c) show the sound pressure level variation and the phase difference, respectively, across the range of operating Mach numbers as reported. Figure 8(b) shows the variation of the screech frequency with the fully expanded jet Mach number. As seen from the figures, there appears to be no switch in the spanwise phase difference at any of the fully expanded Mach numbers and the jets appear to be antisymmetrically coupled over the entire operating range. Figure 8(d) shows the variation of the nonlinear interaction density in the operating range of fully expanded Mach numbers. There is no peak in the nonlinear interaction density. Further confirmation of these results was obtained for the case of twin, shock-containing plane jets with uniform shock cells yawed at 20°. In the interest of brevity, the figures for this case have not been shown. However, it was observed that the coupling instability mode for this case remained antisymmetric for the entire operating range with no mode switch. As expected, the nonlinear interaction density metric did not show any significant peaks. Thus, it appears that when there is no change in the spanwise coupling instability mode over a given operating range, there is no significant increase in the nonlinear interactions across that operating range.

b. Single, shock-containing rectangular jet with uniform shock cells. We examined one last case for a single, shock-

containing plane jet. The microphones were placed on the spanwise extremities, as shown in the schematic in Fig. 2(b). Figure 9(a) shows the variation of the SPL recorded by the two microphones and Fig. 9(c) shows the phase difference between the spanwise instabilities. Figure 9(b) shows the variation in the screech frequency with the Mach number. As seen, there is only one instability mode for the entire range of fully expanded Mach numbers and that is the spanwise symmetric mode. Figure 9(d) shows the variation of the nonlinearities across the Mach number range as indicated by the interaction density. Here too, similar to the result obtained in the previous paragraph, it was seen that when the spanwise instability mode did not exhibit a mode switch, there was no significant increase in the number of nonlinear interactions.

3. Frequency variations during mode jumps

An interesting observation that surfaces from looking at the instability frequency data for each of the flow situations [Figs. 5(c)–9(c)] is the behavior of the frequency variation at or near the mode switch or mode decay. Figures 5(c), 6(c) and 7(c) are the flow situations that exhibit an abrupt mode switch or mode decay. It is seen that in the vicinity of this switch/decay, there is an adjustment in the frequency variation. Where, prior to the switch/decay, the frequency varies smoothly with the Mach number, there seems to be an abrupt shift or discontinuity in the frequency variation once the mode switches. On the other hand, from Fig. 8(c), it can be seen that such a discontinuity in the frequency and SPL variation (around $M_j=1.52$) can occur even when there is no mode switch as seen from the phase data in Fig. 8(d). Thus the variation in the instability frequency or SPL data alone

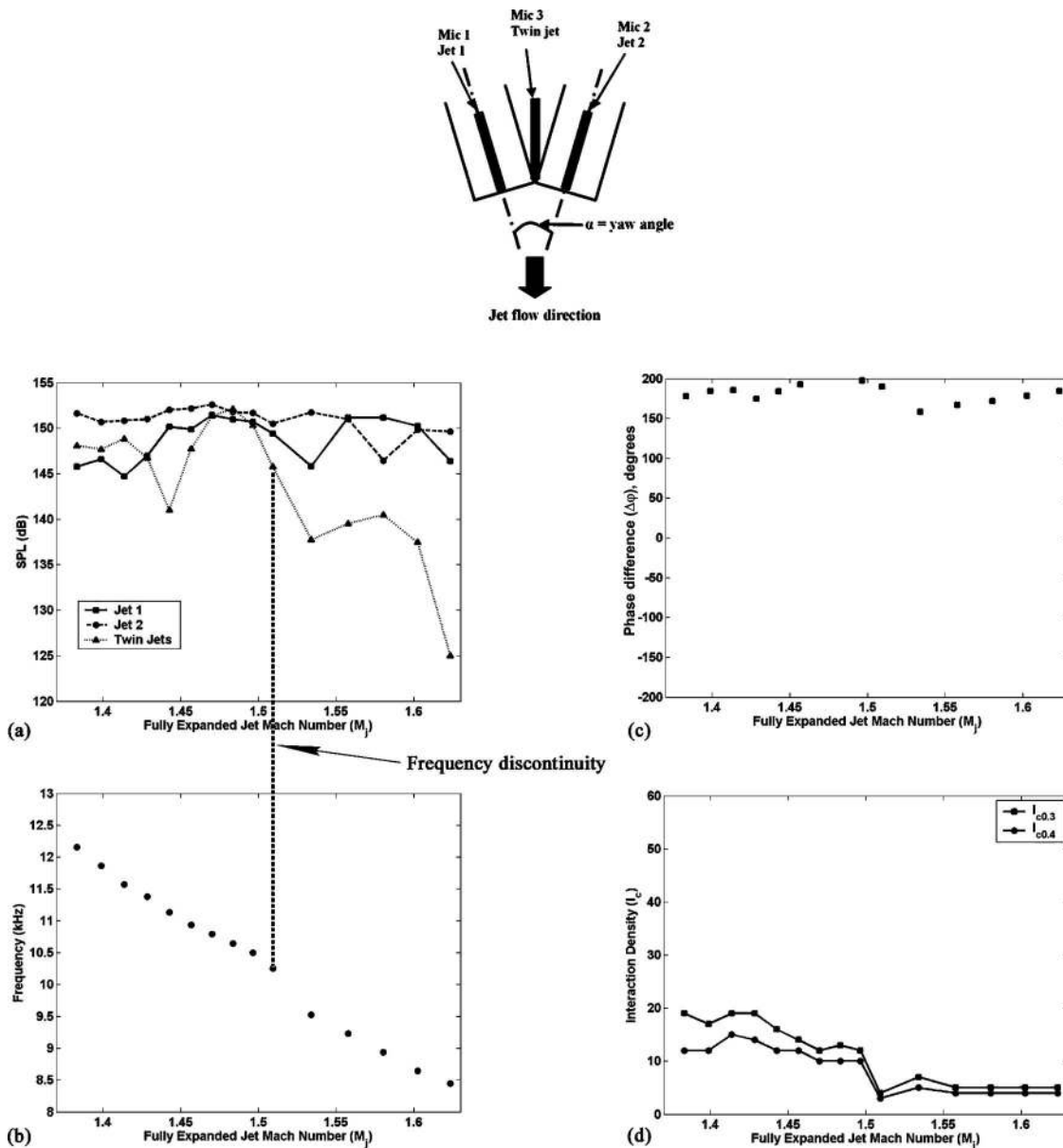


FIG. 8. Linear and nonlinear characteristics of twin jets from uniform exit rectangular nozzles at a yaw angle of 15° . Data from Joshi, Srinivasan, and Raman (Ref. 25) for (a) and (b). (a) Peak SPL variation across the Mach number range for single and twin jets. Single jet data acquired by operating each jet individually and recording the SPL from the corresponding microphone. Twin-jet data acquired by operating both jets simultaneously and recording the SPL from microphone 3. (b) Variation of screech frequency with Mach number. (c) Variation of the spanwise instability mode as measured by microphone 1 and microphone 2 showing the spanwise antisymmetric mode persisting for the entire Mach number range. (d) Variation of nonlinear interaction density with the Mach number for two different cross-bicoherence cutoffs.

would not be sufficient in predicting the presence of a mode switch/decay; the variation of the nonlinear interaction density metric is a faithful indicator and precursor of the presence of a mode switch/decay.

4. Mode switching, nonlinear interactions, and their association with energy exchange

We demonstrated for three separate flow geometries with shock cells that the increase in the number of nonlinear interactions is a precursor to mode switching. The observation that when there was no change in the instability mode the nonlinearities remained at comparable levels across the entire Mach number range lent further credibility to this con-

clusion. Further, for the cases where different instability modes coexist, the decay of one mode and the persistence of another also lead to a sharp increase in the nonlinear interactions. This was demonstrated for the case of an axisymmetric jet with multiple modes that coexisted over the full range of Mach numbers. This sudden increase in nonlinear interactions during abrupt mode switching and/or mode decaying can be expected to be related to energy exchange mechanisms between the instabilities. Linear theory accounts only for energy exchange between the mean flow and the perturbation. However, the energy exchange amongst instability modes can occur only through nonlinear mechanisms. These energy exchange mechanisms manifest as an increase

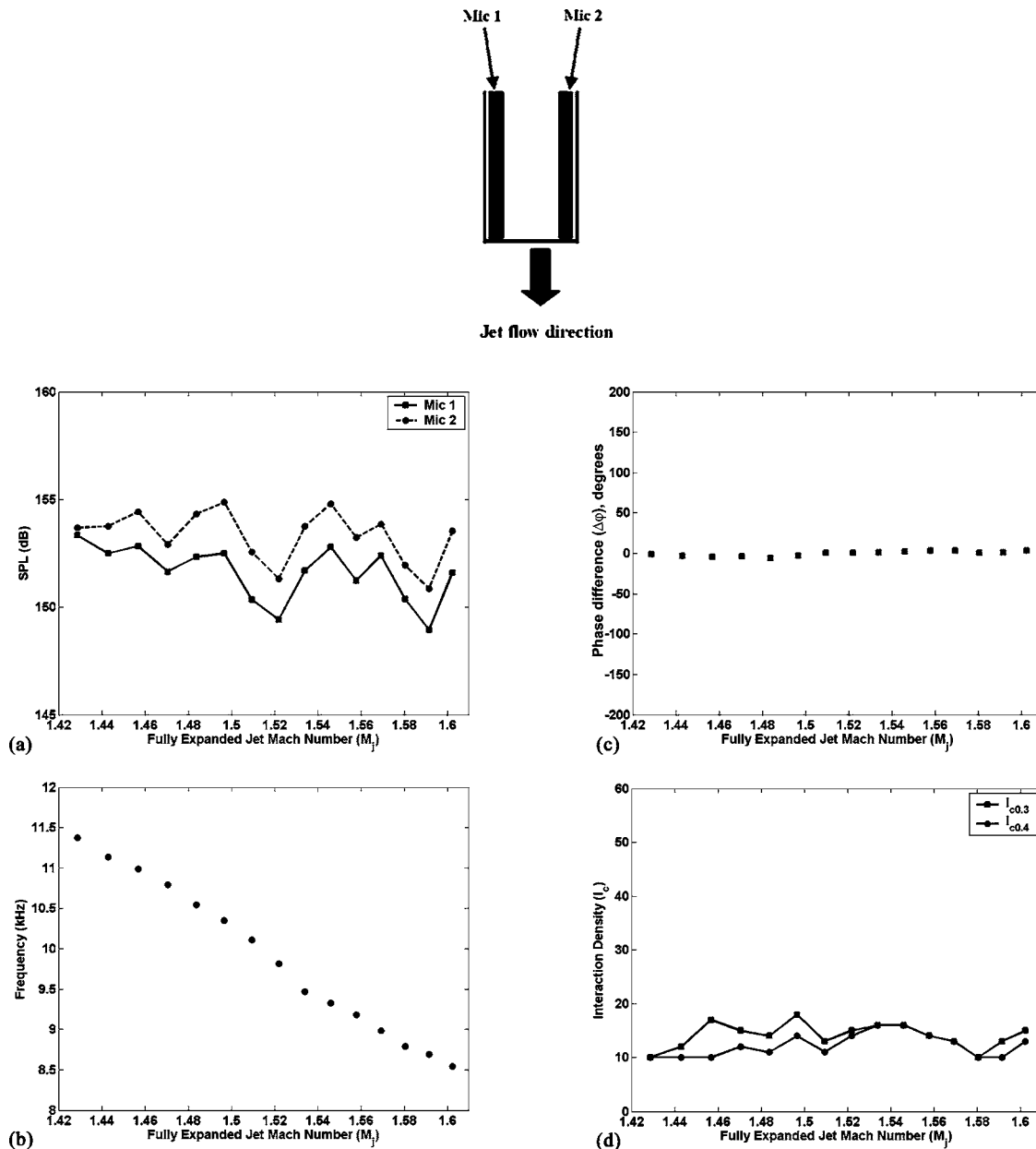


FIG. 9. Linear and nonlinear characteristics of a jet from a uniform exit rectangular nozzle. (a) Peak SPL variation across the Mach number range for spanwise-located microphones as shown in the schematic. (b) Variation of screech frequency with Mach number. (c) Spanwise phase variation between microphone 1 and microphone 2 with Mach number depicting the spanwise symmetric instability mode which persists for the entire Mach number range. (d) Variation of nonlinear interaction density with Mach number for two different cross-bicoherence cutoffs.

in the number of nonlinear interactions during or just around the operating condition where the instability mode changes. From the definition of cross bicoherence it is clear that its magnitude is directly related to the magnitude of energy possessed by the quadratically phase-coupled modes. Thus, quadratic phase coupling can be believed to serve as an energy exchange channel during modal transitions. In the case of plane jets where these instability modes are mutually exclusive, there is a sudden increase in the number of nonlinear interactions (which in our case is quantified by the interaction density term) around the fully expanded Mach number where the switch occurs. On the other hand, in the case of axisymmetric jets where instability modes can coexist, there is a small increase in the number of nonlinear interactions

when one instability mode (in our case the flapping mode) decays and a second (the helical mode) comes into existence while the third (the axisymmetric mode) coexists with the first and the second. However, when there is only one mode that persists, the other one decaying out, there is a prominent and sharp increase in the number of nonlinear interactions.

B. Dominance of difference interactions over sum interactions

Previous studies by Thomas and Chu²⁶ and Srinivasan, Panickar, Raman, Kim, and Williams²⁹ on two entirely different flow situations, reported that in a given cross-bicoherence spectrum, there were a greater number of differ-

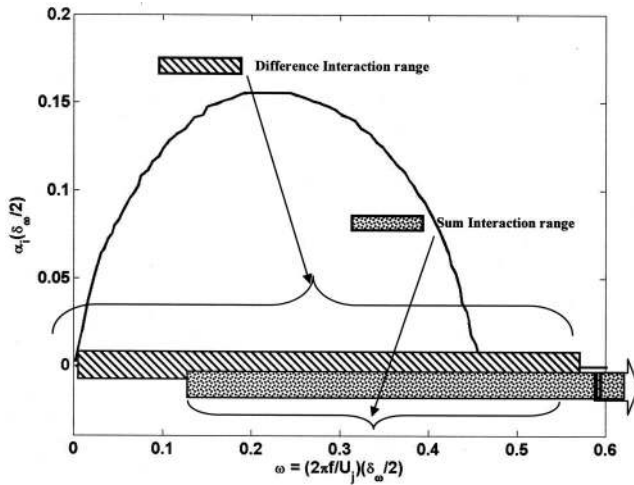


FIG. 10. Band of most amplified instability waves according to linear stability theory. Raman (Ref. 19) [from calculations by Cain and Bower (Ref. 30) and Cain, Bower, Walker, and Lockwood (Ref. 31)] for plane jets at a fully expanded Mach number, $M_j = 1.5$. The nondimensional frequencies that lie within the region where the spatial growth factor [$\alpha_i(\delta_w/2)$] is positive, are unstable and are amplified according to linear stability theory. The shaded area around the X axis shows the range of nondimensional frequencies of the sum and difference interactions obtained from a typical cross-bicoherence spectrum for twin shock-containing coupled jets with uniform exit geometry.

ence interactions than sum interactions. The former paper considered low-speed flows whereas the latter focused on shock-containing flows. We decided to look at the experimental data in the context of linear stability theory, hoping that it would offer a suitable explanation. A single fully expanded jet Mach number of 1.5 was selected for closer study. Figure 10 shows the amplification curve for this case (taken from Raman¹⁹). This curve shows the nondimensional frequencies on the X axis and the spatial instability growth rate on the Y axis. It must be noted that this curve is unique for the operating Mach number and any change in the Mach number will yield a different amplification curve. Frequencies that lie in the range where the spatial growth rate is positive, are unstable, and are amplified in the shear layer. On the other hand, the frequencies that lie outside this range are stable and the disturbances that correspond to this frequency are eventually damped out. For the calculations, a hyperbolic tangent type of velocity profile of the form shown in Eq. (5) was used. The temperature profile that was used is shown in Eq. (6):

$$\frac{U}{U_j} = \frac{1}{2} \left[1 - \tanh \left(\frac{y - y_0}{\frac{1}{2} \delta_w} \right) \right], \quad (5)$$

$$\frac{T}{T_j} = \frac{T_\infty}{T_j} + \frac{1}{2} \left(1 - \frac{T_\infty}{T_j} \right) \left[1 - \tanh \left(\frac{y - y_0}{\frac{1}{2} \delta_w} \right) \right]. \quad (6)$$

In the two equations, U and T are the velocity and temperature, respectively, U_j and T_j are the exit jet centerline velocity and temperature, respectively, y is the smaller dimension coordinate, y_0 is the location of the velocity inflection point in the shear layer, δ_w is the vorticity thickness which was calculated midway between the third and fourth

shocks in the jet exit plume, and T_∞ is the freestream temperature. The original stability calculations for the mean flow as defined in Eqs. (5) and (6) can be obtained from Cain and Bower³⁰ and Cain, Bower, Walker, and Lockwood.³¹ The stability calculations that correspond to the amplification envelope shown in Fig. 10 are for the location where $2y_0/\delta_w = 2$, which is the fully developed region.

For a given cross-bicoherence spectrum, the interacting frequencies and the cross-bicoherence values are stored in a table. Next, it is necessary to obtain the resultant frequency and nondimensionalize it. The nondimensional frequency is given by $\omega = 2\pi f \frac{1}{2} \delta_w / U_j$, where f is the resultant frequency of the nonlinear interactions in hertz. The centerline jet velocity at the exit was calculated using the Mach number and the speed of sound (assuming ambient conditions). Finally, $\frac{1}{2} \delta_w$ was calculated by scaling the values for the jets used by Raman¹⁹ for the jets used in this study. There was a choice of scaling parameters that could be selected, namely, the screech frequency or the smaller dimension of the jets. The value of the vorticity thickness for the jets used in this study that was obtained using the two scaling parameters agreed to within 2%. Thus the experimental data and the stability and experimental results from Raman¹⁹ have been consistently scaled in order to yield a meaningful comparison. Table III shows some sample values of the nondimensional frequencies for the interacting frequencies as well as for the resultant frequency for the case of the twin, shock-containing plane jets with oblique shock cells oriented at a yaw angle of 10° . From Fig. 10 it can be seen that for a Mach 1.5 jet, the cut-off value for the nondimensional frequencies that are amplified is around 0.47. This means that all resultant nondimensional frequencies that are greater than 0.47 are stable and those less than 0.47 are unstable. The rows in Table III shown italicized and in bold font indicate interactions that are unstable.

We analyzed the case of twin, shock-containing plane jets with oblique shock cells. The jets exhausted from nozzles with beveled exits at a bevel angle of 10° , arranged in the contradirected configuration, oriented at a yaw angle of 10° , and operated at a fully expanded jet Mach number of 1.5. Figure 11(a) shows a three-dimensional view of the cross-bicoherence spectrum of this configuration. To facilitate understanding, a projection of the spectrum as viewed from the top is shown in Fig. 11(b). As seen, there are regions of intense clustering of interactions that can be seen in the cross-bicoherence spectrum, which is indicative of a large number of non-linear interactions. The first row of Table IV summarizes the number of nonlinear interactions occurring in the spectrum, sum and difference, and the stability of these interactions. It can be clearly seen that the difference interactions outnumber the sum interactions by more than a factor of 2. Moreover, most of the difference interactions are unstable, roughly 84% of them. On the other hand, most of the sum interactions, around 69%, are stable. As explained earlier, stable interactions lie outside the amplification envelope and are hence damped out whereas the unstable interactions are amplified and become increasingly

TABLE III. Sample constituent and resultant frequencies (dimensional and nondimensional) for coupled twin shock-containing single beveled jets (bevel angle=10°) in contradirected configuration at a yaw angle of 20° and fully expanded Mach number $M_j=1.5$. The amplified interactions are shown in bold type and italicized.

f_1 (Hz)	f_2 (Hz)	$f_{\text{resultant}}$ (Hz)	CBC	ω_1	ω_2	$\omega_{\text{resultant}}$
42 270.06	-31 910.04	10 360.02	0.300	0.726	-0.548	0.178
42 270.06	-9 224.25	33 045.81	0.301	0.726	-0.158	0.567
20 547.95	18 546.28	39 094.23	0.303	0.353	0.318	0.671
42 172.21	1 043.02	43 215.24	0.304	0.724	0.018	0.742
40 215.26	-39 146.02	1 069.24	0.304	0.690	-0.672	0.018
30 919.77	-9 908.74	21 011.03	0.306	0.531	-0.170	0.361
40 508.81	-30 247.72	10 261.09	0.306	0.695	-0.519	0.176
43 248.53	-1 010.43	42 238.10	0.306	0.742	-0.017	0.725
31 213.31	-10 691.00	20 522.30	0.307	0.536	-0.184	0.352
40 215.26	-30 052.15	10 163.11	0.307	0.690	-0.516	0.174
21 330.72	-11 082.14	10 248.59	0.309	0.366	-0.190	0.176
31 409.00	-10 788.79	20 620.21	0.310	0.539	-0.185	0.354
20 939.33	-10 202.09	10 737.25	0.310	0.359	-0.175	0.184
38 356.16	1 043.02	39 399.19	0.312	0.658	0.018	0.676
41 291.59	-18 611.47	22 680.11	0.312	0.709	-0.319	0.389

unstable. Thus, linear stability theory is able to provide guidance regarding the dominance of difference interactions in the given cross-bicoherence spectrum.

Next, we analyzed the data pertaining to the case where the twin-jet configuration was the same as discussed in the preceding paragraph but for a yaw angle of 20°. Figures

12(a) and 12(b) show the three-dimensional and projected cross-bicoherence spectrum, respectively, for this case. As seen from the spectrum, there were a large number of nonlinear interactions in this case as well. However, as opposed to the intense clustering that was seen for the previous case, the clustering in this case was not as intense and additionally,

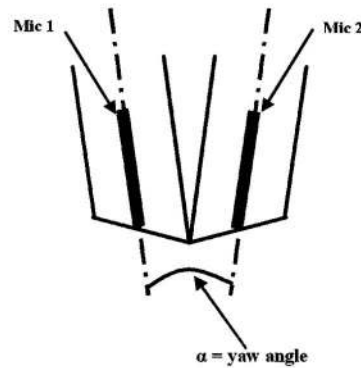
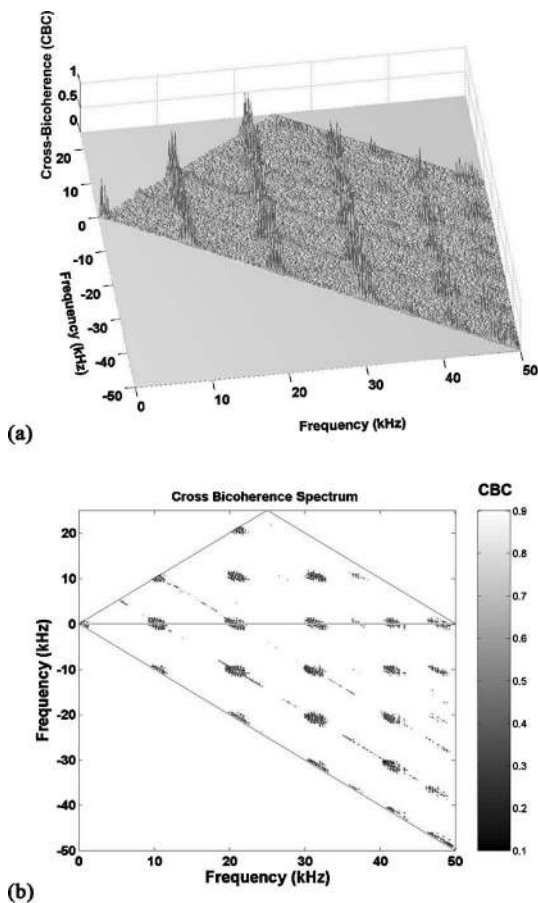


FIG. 11. Spanwise cross-bicoherence for twin single beveled nozzles (bevel angle=10°, yaw angle=10°) in the contradirected configuration operating at $M_j=1.5$. Cross-bicoherence measured using microphones 1 and 2 as shown in the schematic. (a) Three-dimensional representation of the cross-bicoherence spectrum showing the interacting frequencies and the cross-bicoherence magnitude. (b) Top view of the cross-bicoherence spectrum shown in (a). Note the regions of intense clustering, which is indicative of numerous frequencies within close vicinity of each other interacting nonlinearly.

TABLE IV. Summary of interaction types for various flow situations. The corresponding cross-bicoherence spectra for the first two rows of the table are shown in Figs. 11 and 12.

Flow situation	Total sum interactions	Total difference interactions	Sum interaction breakup		Difference interaction breakup	
			Stable	Unstable	Stable	Unstable
Twin contradirected single beveled rectangular jets (bevel angle=10°) at a yaw angle of 10°	106	226	73 (68.87%)	33 (31.13%)	37 (16.37%)	189 (83.63%)
Twin contradirected single beveled rectangular jets (bevel angle=10°) at a yaw angle of 20°	72	131	48 (66.7%)	24 (33.3%)	25 (19.08%)	106 (80.92%)
Twin uniform exit rectangular jets at no yaw	32	75	20 (62.5%)	12 (37.5%)	14 (18.67%)	61 (81.33%)

there were lineal patterns observed in the cross-bicoherence spectrum. This is indicative of the fact that the dominant interactions that occurred were between the screech frequency and its harmonics. The interested reader is referred to the work of Srinivasan, Panickar, Raman, Kim, and

Williams²⁹ for a more detailed explanation of the clustering and lineal interactions. The second row of Table IV summarizes the number and nature of each type of interactions corresponding to the cross-bicoherence spectrum of Fig. 12. In this case too, as with the previous case, the difference inter-

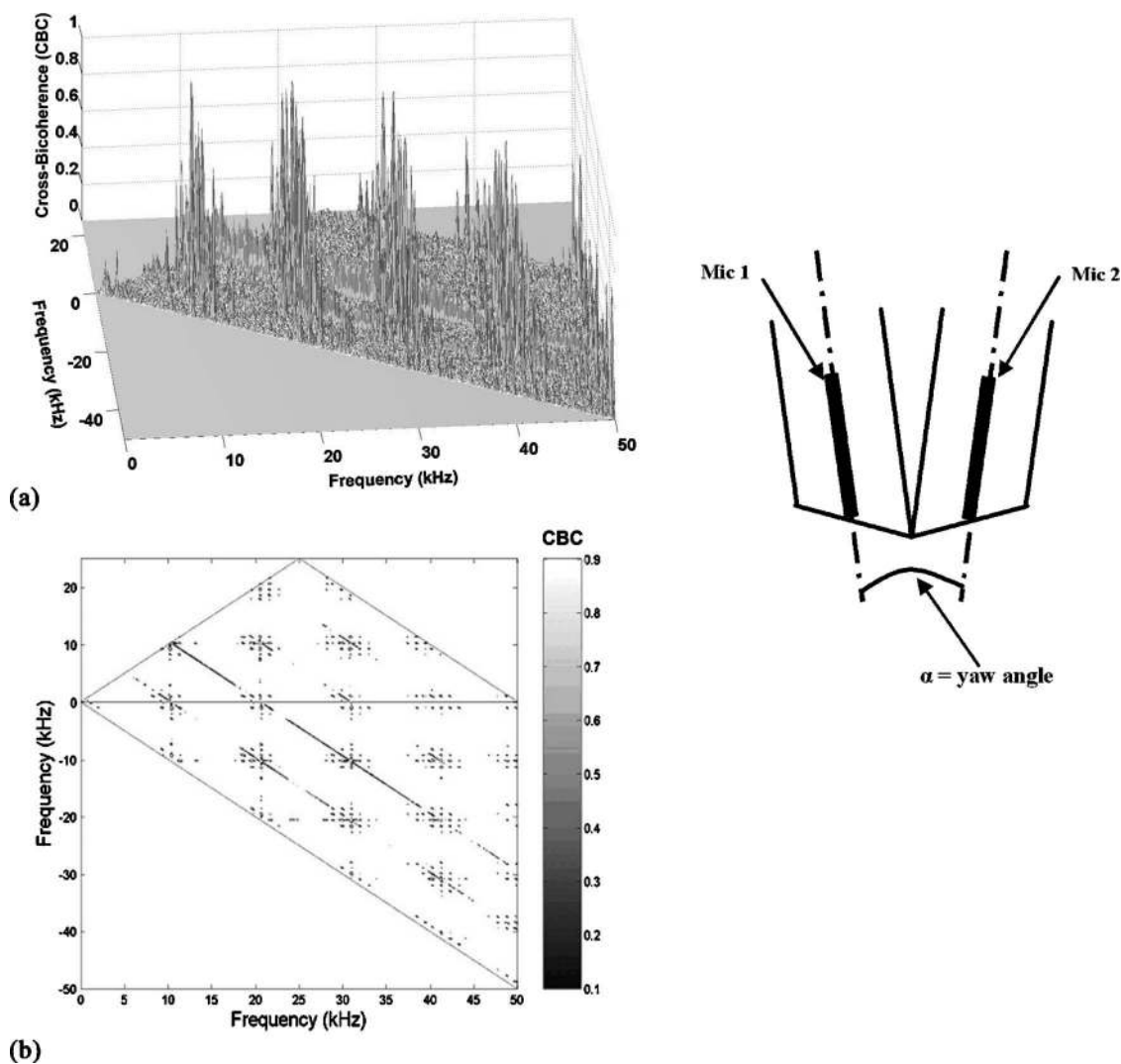


FIG. 12. Spanwise cross-bicoherence for twin single beveled nozzles (bevel angle=10°, yaw angle=20°) in the contradirected configuration operating at $M_j=1.5$. Cross-bicoherence measured using microphones 1 and 2 as shown in the schematic. (a) Three-dimensional representation of the cross-bicoherence spectrum showing the interacting frequencies and the cross-bicoherence magnitude. (b) Top view of the cross-bicoherence spectrum shown in (a). Note the predominantly lineal patterns of nonlinear interactions which is indicative of one strong resultant frequency for all the nonlinear interactions (in this case the screech frequency and its harmonics).

actions outnumber the sum interactions approximately by a factor of 2. Moreover, the resultant frequencies of around 81% of the nonlinear interactions that occurred lay within the amplification envelope and were, hence, unstable. On the other hand, around 67% of the sum interactions were stable. Finally, data for twin, shock-containing plane jets with uniform shock cells were analyzed. However, the spectra for this case have not been shown in the interest of brevity. The third row of Table IV summarizes the number and nature of the interaction types. Again, the difference interactions outnumber the sum interactions by a factor of 2. The trends that were observed in the previous cases repeat here as well in the sense that around 63% of the sum interactions are stable and around 80% of the difference interactions are unstable.

Thus, linear stability theory is able to give a clear indication as to what type of nonlinear interaction is more likely to be seen in a cross-bicoherence spectrum. The difference interactions that occur between two frequencies result in the production of a lower resultant frequency whereas the sum interactions would produce a higher resultant frequency. Lower frequencies are more likely to be unstable, as they are likely to lie within the amplification envelope, as compared to the higher frequencies which would potentially lie outside the envelope and would be damped out.

IV. CONCLUSIONS

In this paper we examined the connection between the number of nonlinear interactions and mode jumps in resonant acoustics situations involving supersonic jets. The use of nonlinear techniques for studying shock-containing jets reveals information that cannot be obtained through linear techniques alone. The application of linear theory is restrictive because it can only explain the exchange of energy between the mean flow and a single perturbation mode. However, the energy exchange between instability modes themselves (without the involvement of the mean flow) can only be explained using the nonlinear theory.

We examined a number of resonant acoustics flow situations with varying flow features: (i) single, shock-containing jet with a two-dimensional exit; (ii) twin, shock-containing jets with two-dimensional exits; and (iii) single, shock-containing jet with an axisymmetric exit. It is known from previous studies that (i) exhibits spanwise instability modes that can be symmetric or antisymmetric, (ii) exhibits spanwise coupling instability modes that can be symmetric or antisymmetric, and (iii) exhibits azimuthal instability modes that can be axisymmetric, flapping, or helical in nature that can coexist. Despite the differences in flow features and geometry exhibited by each of the flow situations just described, there was a unifying factor regarding their behavior during mode switch. It was found that for all cases studied, a sudden increase in nonlinear interactions indicated the presence of a mode switch or mode decay. This was true regardless of the threshold strength chosen for the nonlinear interactions. Thus, the nonlinear interaction density metric serves as a faithful indicator of the presence of a mode switch or mode decay. This is further validated by the fact that when there is no mode switch (uniform exit plane jets)

or there is a coexistence of modes (axisymmetric jets) the interaction density remains at approximately constant values. We believe that when one type of instability mode ceases to exist, it can transfer its energy to another type of instability mode (plane jets) or to the already preexisting instability mode (axisymmetric jets) and this transfer is indicated by observing the trend of the interaction density metric.

The use of linear analysis is, however, able to provide a reasonable explanation as to why difference interactions in a given cross-bicoherence spectrum significantly outnumber the sum interactions. Using the amplification envelope for the instabilities, it can be seen that almost 80% of the difference interactions that occur are unstable. Unstable interactions are the ones that grow spatially in the shear layer and show up consistently in the power spectrum. On the other hand, around 2/3 of the sum interactions are stable, which means that they decay spatially and eventually die out.

ACKNOWLEDGMENT

This work was funded by the U.S. Air Force Office of Scientific Research (AFOSR) with Dr. John Schmisser as Program Manager. Dr. K. Srinivasan was a visiting Assistant Professor at IIT, Chicago, during the performance of this effort.

- ¹A. Powell, "On the noise emanating from a two-dimensional jet above the critical pressure," *Aeronaut. Q.* **4**, 103 (1953).
- ²G. Raman, "Advances in understanding supersonic jet screech: Review and perspective," *Prog. Aerosp. Sci.* **34**, 45 (1998).
- ³A. Powell, "On the mechanism of choked jet noise," *Proc. Phys. Soc. London, Sect. B* **66**, 1039 (1953).
- ⁴M. Merle, "Sur les fréquences des sondes émises par un jet d'air à grande vitesse," *Acad. Sci., Paris, C. R.* **243**, 490 (1956).
- ⁵A. Powell, Y. Umeda, and R. Ishii, "Observations of the oscillation modes of choked circular jets," *J. Acoust. Soc. Am.* **92**, 2823 (1992).
- ⁶T. D. Norum, "Screech suppression in supersonic jets," *AIAA J.* **21**, 235 (1983).
- ⁷J. M. Seiner, J. C. Manning, and M. K. Ponton, "Dynamic pressure loads associated with twin supersonic plume resonance," *AIAA J.* **26**, 954 (1988).
- ⁸R. W. Wlezién, "Nozzle geometry effects on supersonic jet interaction," *AIAA Paper No. 87-2694* (1987).
- ⁹L. Shaw, "Twin-jet screech suppression," *J. Aircr.* **27**, 708 (1990).
- ¹⁰G. L. Morrison and D. K. McLaughlin, "Instability process in low Reynolds number supersonic jets," *AIAA J.* **18**, 793 (1980).
- ¹¹T. F. Hu and D. K. McLaughlin, "Flow and acoustic properties of low Reynolds number underexpanded supersonic jets," *J. Sound Vib.* **141**, 485 (1990).
- ¹²K. B. Yüceil, M. V. Ötügen, and E. Arik, "Underexpanded sonic jets: A PIV study," *Tenth International Symposium on Application of Laser Techniques to Fluid Mechanics, Lisbon, Portugal, 10-13 July 2000*.
- ¹³B. Thurow, J. Hileman, M. Samimy, and W. Lempert, "A technique for real-time visualization of flow structure in high speed flows," *Phys. Fluids* **14**, 3449 (2002).
- ¹⁴K. B. Yüceil and M. V. Ötügen, "Scaling parameters for underexpanded supersonic jets," *Phys. Fluids* **14**, 4206 (2002).
- ¹⁵K. B. M. Q. Zaman, "Asymptotic spreading rate of initially compressible jets—Experiments and analysis," *Phys. Fluids* **10**, 2652 (1998).
- ¹⁶G. Raman, "Screech tones from rectangular nozzles with spanwise oblique shock-cell structures," *J. Fluid Mech.* **330**, 141 (1997).
- ¹⁷G. Raman and E. J. Rice, "Instability modes excited by natural screech tones in a supersonic rectangular jet," *Phys. Fluids* **6**, 3999 (1994).
- ¹⁸C. K. W. Tam, H. Shen, and G. Raman, "Screech tones of supersonic jets from bevelled rectangular nozzles," *AIAA J.* **35**, 1119 (1997).
- ¹⁹G. Raman, "Cessation of screech in underexpanded jets," *J. Fluid Mech.* **336**, 69 (1997).
- ²⁰J. H. Kim and M. Samimy, "Mixing enhancement via nozzle trailing edge

- modifications in a high speed rectangular jet,” *Phys. Fluids* **11**, 2731 (1999).
- ²¹C. Kerechanin, M. Samimy, and J.-H. Kim, “Effects of nozzle trailing edges on acoustic field of a supersonic rectangular jet,” *AIAA J.* **39**, 1065 (2001).
- ²²G. Raman and R. R. Taghavi, “Coupling of twin rectangular supersonic jets,” *J. Fluid Mech.* **354**, 123 (1998).
- ²³G. Raman, “Coupling of twin supersonic jets of complex geometry,” *J. Aircr.* **36**, 743 (1999).
- ²⁴P. Panickar, K. Srinivasan, and G. Raman, “Aeroacoustic features of coupled twin jets with spanwise oblique shock-cells,” *J. Sound Vib.* **278**, 155 (2004).
- ²⁵R. Joshi, K. Srinivasan, and G. Raman, “Coupling of twin jets of complex geometry: Nozzle orientation effects,” *AIAA Paper No. 2004-3920* (2004).
- ²⁶F. O. Thomas and H. C. Chu, “Nonlinear wave coupling and subharmonic resonance in planar jet shear layer transition,” *Phys. Fluids A* **5**, 630 (1993).
- ²⁷M. K. Ponton and J. M. Seiner, “Acoustic study of B helical mode for choked axisymmetric nozzle,” *AIAA J.* **33**, 413 (1995).
- ²⁸S. H. Walker and F. O. Thomas, “Experiments characterizing nonlinear shear layer dynamics in a supersonic rectangular jet undergoing screech,” *Phys. Fluids* **9**, 2562 (1997).
- ²⁹K. Srinivasan, P. Panickar, G. Raman, B.-H. Kim, and D. Williams, “Study of supersonic twin jet coupling using higher order spectral analysis,” *AIAA Paper No. 2003-3871* (2003).
- ³⁰A. B. Cain and W. W. Bower, “Modeling supersonic jet screech: Differential entrainment and amplitude effects,” *AIAA Paper No. 1996-0916* (1996).
- ³¹A. B. Cain, W. W. Bower, S. H. Walker, and M. K. Lockwood, “Modeling supersonic jet screech Part I: Vortical instability wave modeling,” *AIAA Paper No. 1995-0506* (1995).

Physics of Fluids is copyrighted by the American Institute of Physics (AIP).
Redistribution of journal material is subject to the AIP online journal license and/or AIP
copyright. For more information, see <http://ojps.aip.org/phf/phfcr.jsp>